Multi-material continuum topology optimization with multiple volume constraints and material nonlinearity

Danilo B. Cavalcanti[1], Sylvia R. M. Almeida[1], Daniel L. Araújo[1]

[1] *School of Civil and Environmental Engineering, Federal University of Goiás*
Av. Universitária, nº1488, Setor Universitário, 74605-220, Goiás/Goiânia, Brazil
danilo.bc@discente.ufg.br, sylvia@ufg.br, dlaraujo@ufg.br

Abstract. Most existing studies in multi-material continuum topology optimization consider linear elastic material models. Since actual materials, in general, display a nonlinear constitutive relation, this paper presents an initial study to evaluate the influence of the material nonlinearity in the solutions obtained using a multi-material topology optimization approach with multiple volume constraints. Material nonlinearity is considered by means of an Ogden-based model or a bilinear model. To achieve this, a Matlab implementation using the educational code for multi-material topology optimization, `PolyMat`, was made. We took advantage of the modular structure of the educational code to make changes mainly in the structural analysis routine and adapt the optimization formulation for the maximization of the stationarity total potential energy. Numerical examples are presented to demonstrate the influence of material nonlinearity in the optimized topological solutions.

Keywords: Multi-material topology optimization, material nonlinearity.

1 Introduction

The study of multi-material topology optimization is a field that has been getting a lot of interest in the recent years. An interesting aspect of formulations involving multiple materials is the fact that the solution to the optimization problem gives also the optimal material distribution in the optimized structure.

In this paper, we discuss and investigate the distribution of candidate materials with nonlinear elastic behavior in a multi-material topology optimization approach. There is still a limited number of papers that study this specific topic, among which we highlight the works from Zhang, Chi and Paulino [1] and Zhang and Chi [2]. Both works use the virtual element method for the discretization and solution of the variational problem. In this paper, instead, we adopt the finite element method (FEM) for the solution and discretization of the variational problem.

2 Material models

This section presents the material models adopted in this work. Two nonlinear elastic materials were considered: a bilinear material model and a compressible Ogden-based material model.

In this work we assume the hypothesis of small displacements and deformations. The linearized strain tensor ($\boldsymbol{\varepsilon}$) is given by the symmetric part of the gradient of the displacement field.

The response of a material with elastic behavior can be characterized by its strain energy density function (Ψ), since the stress tensor ($\boldsymbol{\sigma}$) and the tangent constitutive tensor ($\boldsymbol{\mathcal{C}}$) are determined as indicated by eq. (1) .

$$\boldsymbol{\sigma}(\boldsymbol{\varepsilon}) = \frac{\partial \Psi}{\partial \boldsymbol{\varepsilon}} \quad \text{and} \quad \boldsymbol{\mathcal{C}}(\boldsymbol{\varepsilon}) = \frac{\partial \boldsymbol{\sigma}(\boldsymbol{\varepsilon})}{\partial \boldsymbol{\varepsilon}} = \frac{\partial^2 \Psi}{\partial \boldsymbol{\varepsilon} \partial \boldsymbol{\varepsilon}}. \tag{1}$$

2.1 Compressible Ogden-based material model

The strain energy density function (Ψ) that defines this material model is given by:

$$\Psi(\lambda_1,\lambda_2,\lambda_3)=\sum_{j=1}^{M}\frac{\mu_j}{\alpha_j}\left(\lambda_1^{\alpha_j}+\lambda_2^{\alpha_j}+\lambda_3^{\alpha_j}-3\right)+\sum_{j=1}^{M}\frac{\mu_j}{\alpha_j\beta_j}\left[J^{-\alpha_j\beta_j}-1\right], \tag{2}$$

where α_j, μ_j, β_j and M are material parameters, $\lambda_i=\overline{\varepsilon}_i+1$, $i=1, 2, 3$ are the principal stretches under small deformations, $\overline{\varepsilon}_i$ is the principal strain and J is the jacobian of the deformation process, defined as $J=\lambda_1\,\lambda_2\,\lambda_3$.

Since the material model is given in terms of the principal strains, it is interesting to write the strain tensor using the spectral decomposition:

$$\boldsymbol{\varepsilon}=\sum_{\alpha=1}^{3}\overline{\varepsilon}_\alpha\mathbf{n}_\alpha\otimes\mathbf{n}_\alpha, \tag{3}$$

where $\mathbf{n}_\alpha$ is the principal direction associated with the principal strain ($\overline{\varepsilon}_\alpha$), and $\otimes$ represents the tensor product operator. Given that the compressible Ogden material model is isotropic, the stress tensor is coaxial with respect to the strain tensor, so the spectral decomposition of the stress tensor can be defined by:

$$\boldsymbol{\sigma}=\sum_{\alpha=1}^{3}\overline{\sigma}_\alpha\mathbf{n}_\alpha\otimes\mathbf{n}_\alpha. \tag{4}$$

Considering the definition presented in eq. (1) and using the strain energy density function from eq. (2), the principal stresses ($\overline{\sigma}_\alpha$) are calculated by eq. (5).

$$\overline{\sigma}_\alpha=\frac{\partial\,\Psi\left(\lambda_1,\lambda_2,\lambda_3\right)}{\partial\,\overline{\varepsilon}_\alpha}=\sum_{j=1}^{M}\mu_j\left(\lambda_\alpha^{\alpha_j-1}-J^{-\alpha_j\beta_j}\lambda_\alpha^{-1}\right). \tag{5}$$

Finally, the tangent constitutive tensor is obtained by the relation between the rate of the stress and the rate of the strain tensors. This derivation is shown in classic continuum mechanics books, the authors highlight the interested readers to consult Holzapfel [3] and Bonet and Wood [4]. Here, for the sake of brevity, we only present the final expression in eq. (6).

$$\mathcal{C}_{OG}=\sum_{\alpha,\beta=1}^{3}\frac{\partial\overline{\sigma}_\alpha}{\partial\overline{\varepsilon}_\beta}\mathbf{n}_\alpha\otimes\mathbf{n}_\alpha\otimes\mathbf{n}_\beta\otimes\mathbf{n}_\beta+\sum_{\substack{\alpha,\beta=1\\ \alpha\neq\beta}}^{3}\frac{1}{2}\frac{\left(\overline{\sigma}_\beta-\overline{\sigma}_\alpha\right)}{\left(\overline{\varepsilon}_\beta-\overline{\varepsilon}_\alpha\right)}\mathbf{n}_\alpha\otimes\mathbf{n}_\beta\otimes\left(\mathbf{n}_\alpha\otimes\mathbf{n}_\beta+\mathbf{n}_\beta\otimes\mathbf{n}_\alpha\right). \tag{6}$$

The derivative in eq. (6) yields:

$$\frac{\partial\overline{\sigma}_\alpha}{\partial\overline{\varepsilon}_\beta}=\sum_{j=1}^{M}\mu_j\left[\left(\alpha_j-1\right)\delta_{\alpha\beta}\lambda_\alpha^{\alpha_j-2}+\delta_{\alpha\beta}\lambda_\alpha^{-2}J^{-\alpha_j\beta_j}+\alpha_j\beta_jJ^{-\alpha_j\beta_j}\lambda_\alpha^{-1}\lambda_\beta^{-1}\right], \tag{7}$$

where $\delta_{\alpha\beta}$ is the Kronecker delta.

2.2 Bilinear material model

The bilinear material model used in this paper is the one presented by Curnier, He and Zysset [5] as a generalization of bimodular material models. The strain energy density function is given by:

$$\Psi(\boldsymbol{\varepsilon})=\frac{1}{2}\lambda(\boldsymbol{\varepsilon})\,\mathrm{tr}^2(\boldsymbol{\varepsilon})+\mu\,\mathrm{tr}(\boldsymbol{\varepsilon}^2), \tag{8}$$

where $\lambda(\boldsymbol{\varepsilon})$ and μ are Lamé's first and second parameters, respectively. The first Lamé's parameter is defined as:

$$\lambda(\boldsymbol{\varepsilon})=\begin{cases}\lambda_c & \text{if } \mathrm{tr}(\boldsymbol{\varepsilon})<0\\ \lambda_t & \text{if } \mathrm{tr}(\boldsymbol{\varepsilon})>0\end{cases}. \tag{9}$$

Note that, in eq. (9), the trace of the strain tensor is the function that divides the space of the infinitesimal

strains. The first Lamé's parameter can be written in terms of the shear modulus and the Young's modulus in tension and compression, as presented in eq. (10)

$$\lambda_c = \frac{\mu\left(E_c - 2\mu\right)}{3\mu - E_c} \quad \text{and} \quad \lambda_t = \frac{\mu\left(E_t - 2\mu\right)}{3\mu - E_t}. \tag{10}$$

The stress tensor and the tangent constitutive tensor are obtained by applying eq. (8) in eq. (1):

$$\boldsymbol{\sigma}\left(\boldsymbol{\varepsilon}\right) = \lambda\left(\boldsymbol{\varepsilon}\right)\,\mathrm{tr}\left(\boldsymbol{\varepsilon}\right)\mathbf{I} + 2\mu\,\boldsymbol{\varepsilon} \quad \text{and} \quad \mathcal{C}_{BL}\left(\boldsymbol{\varepsilon}\right) = \lambda\left(\boldsymbol{\varepsilon}\right)\mathbf{I}\otimes\mathbf{I} + 2\mu\,\boldsymbol{\mathcal{I}}\,, \tag{11}$$

where $\boldsymbol{\mathcal{I}}$ is the symmetric fourth order identity tensor, which is given by $\boldsymbol{\mathcal{I}} = (\delta_{ik}\,\delta_{jl} + \delta_{il}\,\delta_{jk})/2$.

3 Problem formulation

The topology optimization problem considering multiple materials and subjected to multiple volume constraints is presented in eq. (12):

$$\begin{aligned}
&\text{Find:} && \mathbf{z}_1,\ldots,\mathbf{z}_m \\
&\text{That minimizes:} && f\left(\mathbf{z}_1,\ldots,\mathbf{z}_m,\mathbf{U}\right) = -\Pi_{min}\left(\mathbf{z}_1,\ldots,\mathbf{z}_m,\mathbf{U}\right) \\
&\text{Such that:} && g_j\left(\mathbf{z}_1,\ldots,\mathbf{z}_m\right) = \frac{\sum_{i\in\mathcal{G}_j}\sum_{l\in\mathcal{E}_j} A_l\, y_i^{(l)}}{\sum_{l\in\mathcal{E}_j} A_l} - V_{max}^{j} \le 0,\ j = 1,...,nc\,, \\
& && 0 \le z_i^{(e)} \le 1,\ i = 1,\ldots,m \ \text{ e } \ e = 1,...,N \\
&\text{With:} && \mathbf{U}\left(\mathbf{z}_1,\ldots,\mathbf{z}_m\right) = \min_{\mathbf{U}} \Pi\left(\mathbf{z}_1,\ldots,\mathbf{z}_m,\mathbf{U}\right)
\end{aligned} \tag{12}$$

where $\mathbf{z}_i$ is the vector of the design variables associated with material i; $y_i^{(l)}$ is the density of element l associated with material i; f is the objective function, which is the stationary total potential energy, Π_{min}; g_j is the j^{th} volume constraint; $\mathcal{G}_j$ and $\mathcal{E}_j$ are the sets of material and element indices that belong to the j^{th} volume constraint, respectively; V_{max}^{j} is the allowable volume fraction associated with the j^{th} volume constraint; nc is the number of volume constraints; A_l is the volume of element l and $\mathbf{U}$ is the nodal displacement vector which is the solution of the nonlinear elasticity problem.

The element densities are calculated using the density filter proposed by Bourdin [6], with $\mathbf{y}_i = \mathbf{P}\,\mathbf{z}_i$, where $\mathbf{P}$ is the projection matrix. For further explanations about the density filter operator, the authors suggest the readers to check the referred paper.

3.1 Material mixture penalization

We adopted the Discrete Material Optimization (DMO)-type material mixture penalization proposed by Zhang, Chi and Paulino [1]. In this approach, instead of directly interpolating the constitutive tensors, as done in the original DMO-approach, we interpolate the materials' strain energy densities, eq. (13).

$$\Psi_{\rho}^{(e)}\left(z_1^{(e)},\ldots,z_m^{(e)},\mathbf{u}_e\right) = \sum_{k=1}^{m} w_k\left(z_1^{(e)},\ldots,z_m^{(e)}\right)\Psi_k^{(e)}\left(\mathbf{u}_e\right), \text{with } w_k\left(z_1^{(e)},\ldots,z_m^{(e)}\right) = \left(y_k^{(e)}\right)^p \prod_{\substack{r=1\\ r\neq k}}^{m}\left[1-\left(y_r^{(e)}\right)^p\right]. \tag{13}$$

It is worth emphasizing that the interpolation presented in eq. (13) reduces to the original DMO scheme if all candidate materials are linear elastic.

3.2 Nonlinear state equations

The nonlinear state equations are derived from the stationary condition of the total potential energy (Π), defined in eq. (14), which gives the system of nonlinear state equations $\mathbf{F}_{int}(\mathbf{z}_1,\ldots,\mathbf{z}_m,\mathbf{U}) - \mathbf{F}_{ext} = \mathbf{0}$, where $\mathbf{F}_{ext}$ is the external nodal forces vector and $\mathbf{F}_{int}(\mathbf{z}_1,\ldots,\mathbf{z}_m,\mathbf{U})$ is the internal nodal forces vector given by eq. (15).

$$\Pi\left(\mathbf{z}_1,\ldots,\mathbf{z}_m,\mathbf{U}\right)=\sum_{e=1}^{N}\int_{\Omega_e}\Psi_{\rho}^{(e)}\left(z_1^{(e)},\ldots,z_m^{(e)},\mathbf{U}\right)d\Omega_e-\mathbf{F}_{ext}\cdot\mathbf{U}\,. \tag{14}$$

$$\mathbf{F}_{int}\left(\mathbf{z}_1,\ldots,\mathbf{z}_m,\mathbf{U}\right)=\sum_{e=1}^{N}\left\{\sum_{k=1}^{m}w_k\left(z_1^{(e)},\ldots,z_m^{(e)}\right)\int_{\Omega_e}\mathbf{B}_e(\mathbf{x})\cdot\boldsymbol{\sigma}_k^{(e)}(\mathbf{x})\,d\mathbf{x}\right\}, \tag{15}$$

where $\mathbf{B}_e$ is the strain-displacement matrix from the FEM and $\boldsymbol{\sigma}_k^{(e)}$ is the Cauchy stress vector of element e associated to material k. The outer summation indicated in eq.(15) refers to the assemble process related to the finite element method.

To solve the nonlinear system of equilibrium equations, we adopt the Newton-Raphson method with an inexact line-search, presented by Ascher and Greif [7]. It is important to highlight the fact that only material nonlinearity is considered in this paper.

3.3 Sensitivity analysis

The sensitivity of the objective function is given by eq.(16).

$$\frac{\partial f\left(\mathbf{z}_1,\ldots,\mathbf{z}_m,\mathbf{U}\right)}{\partial z_i^{(l)}}=\sum_{e=1}^{N}\frac{\partial f\left(\mathbf{z}_1,\ldots,\mathbf{z}_m,\mathbf{U}\right)}{\partial y_i^{(e)}}\frac{\partial y_i^{(e)}}{\partial z_i^{(l)}}=\sum_{e=1}^{N}P_{el}\frac{\partial f\left(\mathbf{z}_1,\ldots,\mathbf{z}_m,\mathbf{U}\right)}{\partial y_i^{(e)}}, \tag{16}$$

where $\partial y_i^{(e)}\big/\partial z_i^{(e)}=P_{el}$, and P_{el} is the component (e, l) of the projection matrix (**P**). The derivate of the objective function with respect to the element density is given by:

$$\frac{\partial f\left(\mathbf{z}_1,\ldots,\mathbf{z}_m,\mathbf{U}\right)}{\partial y_i^{(e)}}=\sum_{j=1}^{m}\left[\frac{\partial f\left(\mathbf{z}_1,\ldots,\mathbf{z}_m,\mathbf{U}\right)}{\partial w_j\left(z_1^{(e)},\ldots,z_m^{(e)}\right)}\frac{\partial w_j\left(z_1^{(e)},\ldots,z_m^{(e)}\right)}{\partial y_i^{(e)}}\right]+\frac{\partial f\left(\mathbf{z}_1,\ldots,\mathbf{z}_m,\mathbf{U}\right)}{\partial\mathbf{U}}\frac{\partial\mathbf{U}}{\partial y_i^{(e)}}\,. \tag{17}$$

Since the objective function is the stationary total potential energy, the second term on the right-hand side in eq.(17) is zero. So, the sensitivity of the objective function can be calculated with:

$$\frac{\partial f\left(\mathbf{z}_1,\ldots,\mathbf{z}_m,\mathbf{U}\right)}{\partial w_j\left(z_1^{(e)},\ldots,z_m^{(e)}\right)}=-\int_{\Omega_e}\Psi_j^{e}\left(z_1^{(e)},\ldots,z_m^{(e)},\mathbf{U}\right)d\mathbf{x}\,, \tag{18}$$

$$\frac{\partial w_j\left(z_1^{(e)},\ldots,z_m^{(e)}\right)}{\partial y_i^{(e)}}=\begin{cases}p\left(y_i^{(e)}\right)^{p-1}\displaystyle\prod_{\substack{k=1\\k\neq i}}^{m}\left[1-\left(y_k^{(e)}\right)^{p}\right] & ,\,i=j\\ -\left(y_i^{(e)}\right)^{p-1}\left(y_j^{(e)}\right)^{p}\displaystyle\prod_{\substack{k=1\\k\neq i,j}}^{m}\left[1-\left(y_k^{(e)}\right)^{p}\right] & ,\,i\neq j\end{cases}. \tag{19}$$

The sensitivity of the volume constraint j with respect to the design variables is given by:

$$\frac{\partial g_j\left(\mathbf{z}_1,\ldots,\mathbf{z}_m\right)}{\partial z_i^{(l)}}=\sum_{e=1}^{N}\frac{\partial g_j\left(\mathbf{z}_1,\ldots,\mathbf{z}_m,\mathbf{U}\right)}{\partial y_i^{(e)}}\frac{\partial y_i^{(e)}}{\partial z_i^{(l)}}=\sum_{e=1}^{N}P_{el}\left[\frac{A_l}{\sum_{k\in\mathcal{E}_j}A_k}\right]. \tag{20}$$

4 ZPR update scheme

The optimization problem presented in eq. (12) contains multiple volume constraints, which are linear functions of the design variables. In order to efficiently solve the problem, in this work we use the ZPR design variable update scheme proposed by Zhang, Paulino and Ramos Jr. [8]. Originally proposed in the context of the Ground Structure approach, the ZPR design variable update scheme was later adapted by Sanders, Aguiló e Paulino [9] to be used in the density method, with an additional inclusion of the consideration of the Density Filter during the update. This version, "ZPR + Density Filter", is the one provided in the default version of the

educational Matlab code, `PolyMat`, presented by Sanders *et al*. [10], and was used in this paper.

In a brief explanation, the ZPR update scheme is derived by linearizing the objective function using an exponential intermediate variable and applying the optimality condition on the convex approximated optimization problem. By using Lagrangian duality, it can be proven that the Lagrange multipliers are decoupled, allowing the design variables associated to each constraint to be updated in an independent way. For a better explanation about the derivation of these mathematical features, the authors suggest the readers to check the papers from Zhang, Paulino and Ramos Jr. [8], Sanders *et al* [10] and Zhang, Chi and Paulino [2]. For the sake of brevity, we only present the update scheme:

$$z_i^{(e),k+1} = \begin{cases} z_{i,U}^{(e),k}, & z_i^{(e),*} \geq z_{i,U}^{(e),k} \\ z_i^{(e),*}, & z_{i,L}^{(e),k} < z_i^{(e),*} < z_{i,U}^{(e),k} \\ z_{i,L}^{(e),k}, & z_i^{(e),*} \leq z_{i,L}^{(e),k} \end{cases}, \tag{21}$$

where, $z_i^{(e),*}$ is the candidate updated design variable, calculated with eq. (22); $z_{i,U}^{(e),k}$ and $z_{i,L}^{(e),k}$ are the upper and lower move limits, respectively, which are defined as presented in eq. (23). It is worth mentioning that in this context the index k refers to iteration of the optimization process, e refers to the element and i to the material.

$$z_i^{(e),*} = z_{min} + \left(\sum_{l=1}^{N} P_{el} z_i^{(l),k} - z_{min} \right) \left(- \frac{\partial f\left(\mathbf{z}_1^k, \ldots, \mathbf{z}_m^k\right)}{\partial z_i^{(e)}} \Big/ \phi^j \frac{\sum_{l \in \mathcal{E}_j} A_l \, y_i^{(l),k}}{\sum_{l \in \mathcal{E}_j} A_l} \right)^{\eta}. \tag{22}$$

In eq. (22), ϕ^j is the Lagrange multiplier associated with constraint j and η is the damping factor, that usually is assumed as 0.5 and M is the ZPR move parameter, which was assumed as 0.2.

$$\begin{cases} z_{i,L}^{(e),k} = \max\left(z_{min}, z_i^{(e),k} - M\right) \\ z_{i,U}^{(e),k} = \min\left(1, z_i^{(e),k} + M\right) \end{cases}, \tag{23}$$

5 Numerical results

In this section, a numerical example is presented to illustrate some of the features of this optimization problem. For all solutions presented, the tolerance of the residual norm is 10^{-6}, the maximum number of iterations of the Newton-Raphson method is set to 30 iterations, the initial value of the radius of the density filter is $R_0 = 0.2$, which is decreased after 150 iterations of the optimization process by 3 $R_0/20$ until it reaches a value equal to $R_0/4$. The SIMP penalization coefficient is initially equals 1 and it is increased by 0.1 every iteration until it reaches a value equal to 3. The optimization process ends when the maximum change of the design variables is smaller than 0.01 or when the number of iterations is bigger than 300. Plane stress condition is assumed.

The computational implementation was made using the educational code provided by Sanders *et al* [10]. The domain was discretized by a Centroidal Voronoi Tessellation (CVT) mesh, with 10000 polygonal finite elements, generated with the use of `PolyMesher`, which is an educational Matlab code presented by Talischi *et al*. [11].

Figure 1 presents the stress-strain behavior in uniaxial test of the 5 candidate materials adopted and Tab. 1 presents the definition of the material models and its associated parameters.

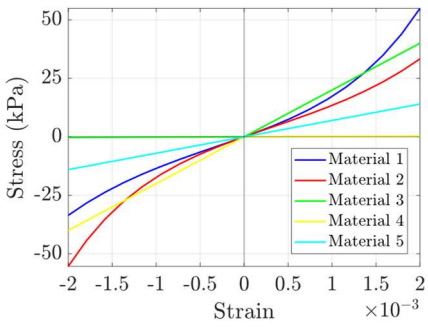

Figure 1. Stress-strain behavior in uniaxial test of the candidate materials

Table 1. Definition of the material model and its associated parameters

Material	Model	Parameters
1	Ogden	[μ, α, β] = [7.6923, 1000, 0.75]
2	Ogden	[μ, α, β] = [-7.6923, -1000, 0.75]
3	Bilinear	[E_t, E_c, G] = [2e4, 125, 7.6923e3]
4	Bilinear	[E_t, E_c, G] = [125, 2e4, 7.6923e3]
5	Bilinear	[E_t, E_c, G] = [7e3, 7e3, 2.6923e3]

The selected numerical example is the Michell cantilever, whose geometry and boundary conditions are presented in Fig. 2. We also present in Fig. 2 two settings of volume constraints (g_j). In the first, Fig. 2(a), one volume constraint is associated with the materials with higher stiffness in tension (materials 1 and 3), one is associated with the materials with higher stiffness in compression (materials 2 and 4), and one is associated with the material with linear behavior (material 5); the second setting, Fig. 2(b), it is defined with one volume constraint per material. Is worth mentioning that the summation of the volume constraints (g_j) in both cases are 35%.

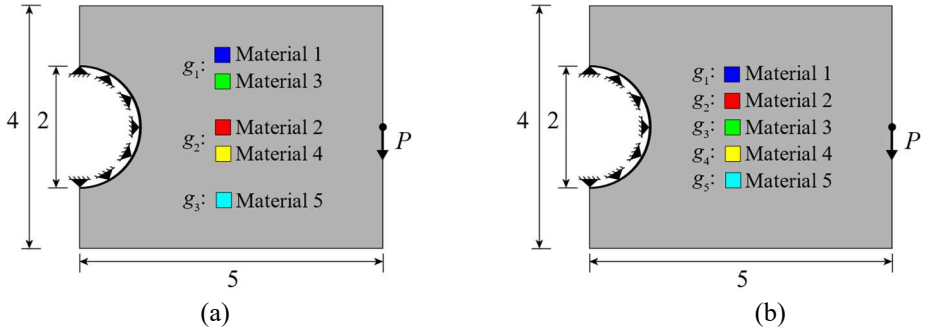

Figure 2. Dimensions, boundary conditions and constraints definitions: (a) Setting 1; (b) Setting 2

The problem for the Setting 1 was solved considering two load levels: $P = 1$ kN (small) and $P = 10$ kN (larger). When only materials with linear behavior are considered, the material distribution and the topology remain the same with the application of different load levels. But, as can be seen in Fig. 3, the topology and the material selection of each member is different. With the small load level, Fig. 3(a), the deformation level is also smaller and the bilinear candidate materials 3 and 4 are stiffer than the Ogden-based candidate materials 1 and 2. Though, as the load level is increased, Fig. 3(b), the Ogden-based candidate materials become stiffer than the bilinear material models. Thus, not only the topology is different, but also the selection of the material in each member of the solution.

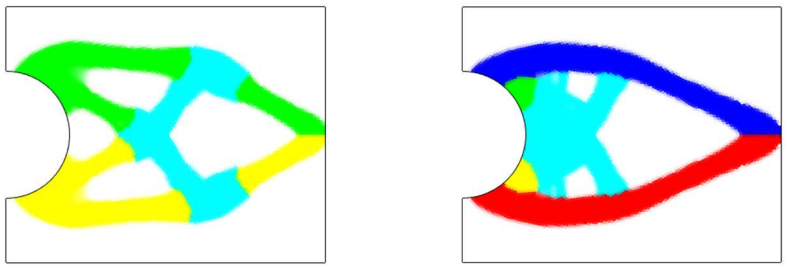

Figure 3. Solutions considering Setting 01 of volume constraints: (a) $P = 1$ kN; (b) $P = 10$ kN

In the Setting 2 a numerical problem happened during the optimization process as the continuation scheme for the radius of the Density Filter began to be reduced for the solution with larger load level. This problem still has to be better investigated, but we tested to solve the problem without the ZPR + Density Filter approach. With this attempt, the problem with both load levels could be solved, although there is a clear decrease in the quality of

the topology solutions, that has yet to be better investigated. Solutions are presented in Fig. 4.

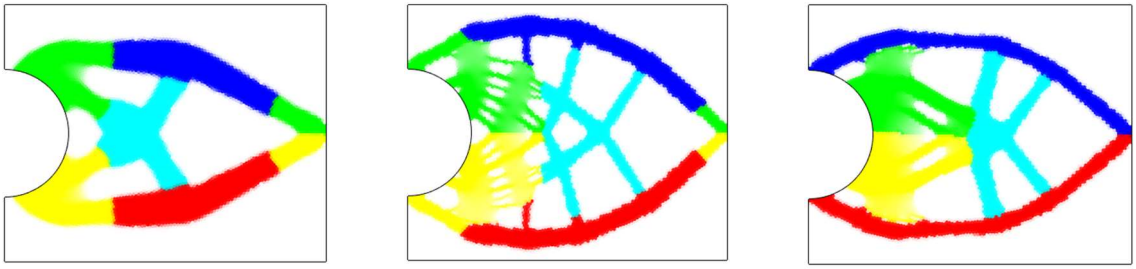

(a) (b) (c)

Figure 4. Solution considering Setting 02 of volume constraints: (a) P = 1 kN (ZPR + Density Filter); (b) P = 1 kN (ZPR only); (b) P = 10 kN (ZPR only);

6 Conclusions

This paper was an initial study about multi-material topology optimization considering candidate materials with nonlinear elastic behavior. The numerical example highlights the fact that the topology and the material selection is load level dependent. Further investigations are needed to explain the numerical instability that occurred in the volume constraint setting 2 for the higher load level. This initial work leaves room for further developments including the extension to other nonlinear elastic models.

Acknowledgements. The authors acknowledge the financial support from CAPES (in Portuguese "Coordenação de Aperfeiçoamento de Pessoal de Nível Superior"). The authors also would like to thank the authors of the `PolyMat` paper for providing the educational code.

Authorship statement. The authors hereby confirm that they are the sole liable persons responsible for the authorship of this work, and that all material that has been herein included as part of the present paper is either the property (and authorship) of the authors, or has the permission of the owners to be included here.

References

[1] X. S. Zhang and H. Chi, "Efficient multi-material continuum topology optimization considering hyperelasticity: Achieving local feature control through regional constraints". *Mechanics Research Communications*, v. 105, p. 46–48, 2020.
[2] X. S. Zhang, H. Chi and G. H. Paulino, "Adaptive multi-material topology optimization with hyperelastic materials under large deformations: A virtual element approach", *Computer Methods in Applied Mechanics and Engineering*, v. 370, p. 112976, 2020.
[3] G. A. Holzapfel. *Nonlinear Solid Mechanics: A Continuum Approach for Engineering*. John Wiley & Sons, 2000.
[4] J. Bonet, J. and R. D. Wood. *Nonlinear Continuum Mechanics for Finite Element Analysis*. 2. Ed, New York: Cambrigde University Press, 2008.
[5] A. Curnier, Q. C. He and P. Zysset, "Conewise linear elastic materials", *Journal of Elasticity*, v. 37, pp. 1-38, 1995.
[6] B. Bourdin, "Filters in topology optimization", *International Journal for Numerical Methods in Engineering*, v. 50, pp. 2143–2158, 2001.
[7] U. M. Ascher, C. Greif. *A First Course in Numerical Methods*. Philadelphia: Society for Industrial and Applied Mathematics, 2011.
[8] X. S. Zhang, G. H. Paulino and A. S. Ramos Jr., "Multi-material topology optimization with multiple volume constraints: a general approach applied to ground structures with material nonlinearity", *Structural and Multidisciplinary Optimization*, v. 57, n. 1, p. 161–182, 2018
[9] E. D. Sanders, M. A. Aguiló and G. H. Paulino, "Multi-material continuum topology optimization with arbitrary volume and mass constraints", *Computer Methods in Applied Mechanics and Engineering*, v. 340, p. 798–823, 2018.
[10] E. D. Sanders, A. Pereira, M. A. Aguiló and G. H. Paulino, "PolyMat: an efficient Matlab code for multi-material topology optimization", *Structural and Multidisciplinary Optimization*, v. 58, n. 6, p. 2727–2759, 2018.
[11] C. Talischi, G. H. Paulino, A. Pereira, I. F. M. Menezes, "PolyMesher: a general-purpose mesh generator for polygonal elements written in Matlab", *Structural and Multidisciplinary Optimization*, v. 45, n. 3, p.309-328, 2012.